J Electr Eng Technol Vol. 9, No. 6: 1873-1881, 2014
http://dx.doi.org/10.5370/JEET.2014.9.6.1873

ISSN(Print) 1975-0102
ISSN(Online) 2093-7423

PSSs and SVC Damping Controllers Design to Mitigate Low Frequency Oscillations Problem in a Multi-machine Power System

Mohsen Darabian† and Abolfazl Jalilvand*

Abstract – This paper deals with the design of multi-machine power system stabilizers (PSSs) and Static var compensator (SVC) using Modified shuffled frog leaping algorithm (MSFLA). The effectiveness of the proposed scheme for optimal setting of the PSSs and SVC controllers has been attended. The PSSs and SVC controllers designing is converted to an optimization problem in which the speed deviations between generators are involved. In order to compare the capability of PSS and SVC, they are designed independently once, and in a coordinated mode once again. The proposed method is applied on a multi-machine power system under different operating conditions and disturbances to confirm the effectiveness of it. The results of tuned PSS controller based on MSFLA (MSFLAPSS) and tuned SVC controller based on MSFLA (MSFLA SVC) are compared with the Strength pareto evolutionary algorithm (SPEA) and Particle swarm optimization (PSO) based optimized PSS and SVC through some performance to reveal its strong performance.

Keywords: Modified shuffled frog leaping algorithm (MSFLA), PSS and SVC design, Multi machine power system, Strength pareto evolutionary algorithm (SPEA), Particle swarm optimization (PSO).

1. Introduction

Owing to the environmental and economic pressures, electric power system becomes more heavily loaded and system oscillations are increased. Inadequate damping of these oscillations will restrict the power transfer capability. The conventional PSS (CPSS) is widely utilized to enhance the system damping. In some cases, if the utilization of PSS cannot provide sufficient damping for inter-area power swing, Flexible AC transmission systems (FACTS) devices are substitute effectual solutions. The principle of these FACTS devices is to regulate the reactance and voltage. SVC is the most popular FACTs device utilized to improve the reliability of power systems [1]. It has different capability to improve the operation of power systems by mitigating network loss, providing voltage regulation, compensating active power, improving transient stability, limiting short circuit currents and damping the power system oscillation [2]. The system damping can be enhanced by incorporating supplemental damping controller.

Numerous schemes have been documented for PSS and SVC parameters optimization to improve the damping of power system oscillations. Genetic algorithms (GA) [3], Tabu search (TS) [4], simulated annealing [5] evolutionary programming [6] have been proposed to design PSS parameters. In [7], an adaptive network based fuzzy inference system (ANFIS) is used to improve the power system damping via SVC. In [8], a new scheme is proposed to find optimal location of SVCs to increase power system stability. In order to increase power system stability, a new scheme based on wide area signals via SVC is suggested in [9]. A BFOA algorithm is used in [10] to design SVC parameters in a single machine infinite bus system. In [11], a pade approximation technique is suggested to design of SVC with delayed input signal. In [12], a hybrid scheme is used to simulate power systems equipped with SVC. A simultaneous tuning of a PSS and a SVC controller based on GA is represented in [13]. The adjusted design of PSSs and SVC based on probabilistic theory is described in [14]. In [15], the decentralized modal control technique is applied to pole placement in multi-machine power system using FACTS devices. In [16], an extensive evaluation is performed on PSS and FACT device independently as well as in a coordinated mode.

In this paper, the problem of PSS and SVC design is formulated as an optimization problem and MSFLA is used to solve it. The objective is to improve the stability of the multi-machine power system, subjected to the disturbance. The capability of the proposed MSFLAPSS and MSFLASVC is tested on a multi-machine power system under different operating conditions in comparison with the PSO [17] and SPEA [18] based tuned PSS and SVC through proper value analysis, nonlinear time simulation and some performance indices. Results evaluation shows that the proposed method achieves significant improvement for stability performance of the system under different operating conditions and is superior to the other methods.

The paper is sets out as follows: Section 2 presents the

† Corresponding Author: Dept. of Electrical Engineering, Univerity of Zanjan. Zanjan, Iran. (m.darabian@znu.ac.ir)
* Dept. of Electrical Engineering, Univerity of Zanjan. Zanjan, Iran. (ajalilvand@znu.ac.ir)
Received: Febuary 3, 2013; Accepted: July 16, 2014

problem formulation. The proposed solution method for the problem is presented in section 3. The application of the proposed method and simulation results are presented in Section 4. Finally, section 5 concludes the paper.

2. Problem Formulation

2.1 Power system model

A power system can be stated by a set of nonlinear differential equations as follow:

$$\dot{X} = f(X,U) \tag{1}$$

The linearized incremental model around an equilibrium point is usually employed in designing of PSS and SVC. Hence, the state equation of a power system with n machines and m PSS and SVC can be formulated as follow:

$$\dot{X} = AX + BU \tag{2}$$

Where X is the state vector and U is the input vector; in this paper $X = [\delta, \omega, E_q', E_{fd}, V_f]^T$ and U is the PSS and SVC output signals; δ and ω are the rotor angle and speed, respectively; E_q', E_{fd} and V_f are the internal, the field, and excitation voltages respectively; A is a $5n*5n$ matrix and equals $\partial f/\partial X$; B is a 5n*m matrix and equals $\partial f/\partial U$; X is a $5n*1$ state vector; U is an m*1 input vector.

2.2 PSS structure

PSS is used to provide an appropriate torque on the rotor of machine to compensate the phase lag between the exciter input and the machine electrical torque. The additional stabilizing signal assumed is one proportional to the speed. The CPSS is contemplated throughout the paper [19]. Fig. 1 depicts the block diagram of the i*th* PSS, where $\Delta\omega_i$ is the deviation in speed from the synchronous speed. This kind of stabilizer comprises of a dynamic compensator and a high pass filter. The output signal is supplied as an additional input signal, U_i to the regulator of the excitation system. The steady state offset in the output of the PSS is reset by the filter. The time constant T_W can usually vary from 0.5 to 20 Sec. The dynamic compensator is constituted of a supplemental gain and a lead lag circuit. The alterable PSS parameters are K_i, T_W, T_{1i}, T_{2i}, T_{3i} and T_{4i}. The phase lead compensation is provided by the lead lag block for the phase lag which is presented in the circuit between the exciter input and the electrical torque.

2.3 SVC structure

The SVC model used in this study is depicted in Fig. 2. The system is connected to the AC system via a transformer to bring the voltages up to the required transmission levels.

Fig. 3 illustrates the block diagram of a SVC with auxiliary stabilizing signal. This controller includes gain block, two stages of lead lag compensator and signal washout block. By controlling the firing angle of the thyristors, the bus voltage magnitude is controlled by SVC:

$$\dot{B}_e = \frac{1}{T_r}[-B_e + Kr(V_{ref} - V_t + V_s)] \tag{3}$$

Where T_r is the time constant and K_r is the gain. demonstrate the thyristors firing control system and the effective susceptance of it stated as follow:

$$B_V = -\frac{2\pi - 2\alpha + \sin 2\alpha}{\pi X_L} \qquad \pi/2 \le \alpha \le \pi \tag{4}$$

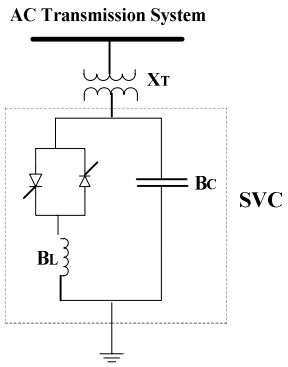

Fig. 2. SVC equivalent circuit

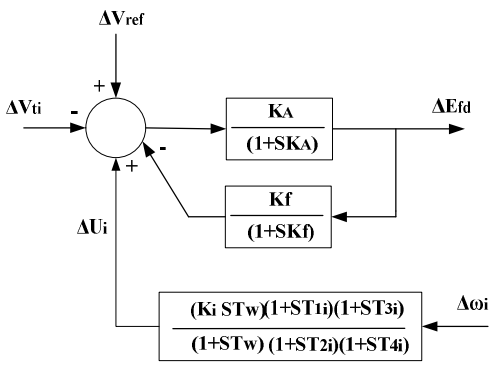

Fig. 1. Block diagram of i*th* PSS

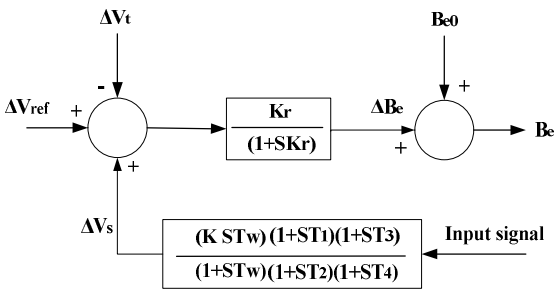

Fig. 3. Block diagram of SVC

Where X_L is the reactance of the fixed inductor of SVC. The effective susceptance of this model is formulated as follow:

$$X_e = X_c \frac{\pi / r_x}{\sin 2\alpha - 2\alpha + \pi(2 - 1/r_x)} \quad (5)$$

Where $X_e = -1/B_e$ and $r_x = X_e/X_L$.

2.4 The system under study

The single line diagram of the test system used in this paper is depicted in Fig. 4 and its data is represented in [20].

The proper values and frequencies connected to the rotor oscillation modes of the system are shown in Table 1.

It is shown in the table, the 0.2371 Hz mode is the inter area mode with G1 oscillating against G2 and G3. The 1.2955 and 1.8493 Hz modes are the inter machine oscillation local to G2 and G3 respectively. Furthermore, the instability of the system is revealed by the positive real part of proper value of G1. Table 2 shows the system and generator loading levels. Two main plans will be demonstrated to find the appropriate place of the SVC in the system. The first strategy is based on investigating the impact of load percentage and the second one is involved with system voltages owing to the line outage [21].

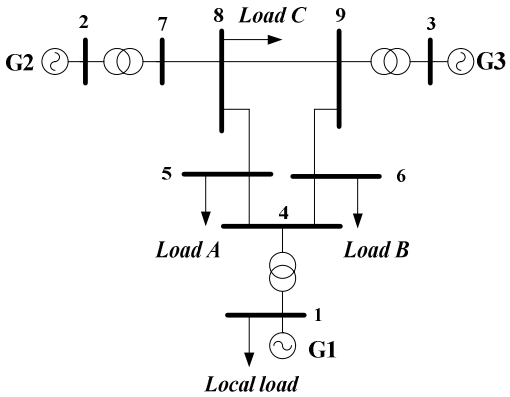

Fig. 4. The system under study

Table 1. The proper values and frequencies connected to the rotor oscillation mode of the system

Generator	Proper values	Frequencies	Damping ratio ζ
G1	+0.15 ± 1.49j	0.2371	-0.1002
G2	-0.35 ± 8.14j	1.2955	0.0430
G3	-0.67 ± 1.62j	1.8493	0.0576

Table 2. Loading condition for the system

Generator	Light		Normal		Heavy	
	P	Q	P	Q	P	Q
G1	0.9649	0.223	1.7164	0.6205	3.5730	1.8143
G2	1.0000	-0.1933	1.630	0.0665	2.20	0.7127
G3	0.4500	-0.2668	0.85	0.1086	1.35	0.4313
Load						
A	0.70	0.350	1.25	0.5	2.00	0.90
B	0.50	0.30	0.9	0.30	1.80	0.60
C	0.600	0.200	1.00	0.35	1.60	0.65
Local load	0.600	0.200	1.000	0.35	1.60	0.65

Table 3. Effect of load percentage on load bus voltage

Load%	0.25	0.5	0.75	1.00	1.25	1.5	1.75
Bus4	1.0573	1.0479	1.0375	1.0258	1.0126	0.9975	0.9799
Bus5	1.0593	1.0403	1.0192	0.9956	0.9691	**0.9389**	**0.9036**
Bus6	1.0643	1.0487	1.0315	1.0127	0.9917	0.9681	**0.9036**
Bus7	1.0500	1.0434	1.0354	1.0258	1.0143	1.0005	0.9839
Bus8	1.0535	1.0425	1.0300	1.0159	0.9998	0.9814	0.9599
Bus9	1.0508	1.0456	1.0395	1.0324	1.0241	1.0144	1.0029

Table 4. Effect of line outage on load bus voltage

Line Outage	4-5	4-6	5-7	6-9	7-8	8-9
Bus4	1.0388	1.0282	0.9956	1.0189	1.0234	0.9994
Bus5	**0.8389**	0.9988	**0.9380**	0.9678	0.9736	0.9897
Bus6	1.0203	**0.9418**	0.9748	0.9678	0.9994	0.9897
Bus7	0.9878	1.0223	1.0170	1.0156	0.9994	1.0100
Bus8	0.9895	1.0063	1.0010	1.0054	0.9994	1.0100
Bus9	1.0244	1.0167	1.0189	1.0234	0.9994	1.0100

The effect of load percentage and line outage on bus voltages of the system are given in Tables 3 and 4. It can be observed that the voltages are influenced remarkably at load buses 5 and 6, respectively. This fact can be arisen from the connection of these buses with the longest lines in the system which possesses bigger resistances and reactances than the others. As a result the buses 5 or 6 can be assumed as the best candidate for the SVC placing. Both candidates are adjacent machine 1 which brings about the system instability owing to its unstable mechanical mode. Additionally, bus 5 is the worst one and will be surmised as the best candidate to install the SVC.

2.5 The fitness equation

The purpose of this paper is optimal coordinated design of PSS and SVC via MSFLA technique. To seek the optimum controller parameters, the design problem can be formulated with the following fitness function based on the Integral of Time Multiple Absolute Error (ITAE) as follow:

$$J = \int_0^\infty t(|\Delta\omega_{12}| + |\Delta\omega_{23}| + |\Delta\omega_{13}|)dt \quad (6)$$

Where $\Delta\omega_{12}=\Delta\omega_1 - \Delta\omega_2$, $\Delta\omega_{23}=\Delta\omega_2 - \Delta\omega_3$ and $\Delta\omega_{13}=\Delta\omega_1 - \Delta\omega_3$.

The major goal is to minimize the J, as follow:

$$FF : Minimize\,(J) \quad (7)$$

In order to reduce the computational difficulty, T_W is assumed 10 sec, T_{2i} and T_{4i} are kept constant at a reasonable value of 0.05 s and adjusting of T_{1i}, T_{3i} and K_i are taken on attaining the system requirement. These parameters are experimentally limited. The computational

Table 5. CPSS boundaries

Generator	T_{1i}	T_{3i}	K_i
Minimum	0.06	0.06	1
Maximum	1.0	1.0	100

difficulty can be notably reduced by these boundaries (Table 5).

3. Shuffled Frog Leaping Algorithm

In the natural memetic evolution of a frog population, the ideas of the worse frogs are influenced by the ideas of the better frogs, and the worse frogs tend to jump toward the better ones for the possibility of having more foods. The frog leaping rule in the shuffled frog leaping algorithm (SFLA) is inspired from this social imitation, but it performs only the jump of the worst frog toward the best one [22]. According to the original frog leaping rule, the possible new position of the worst frog is restricted in the line segment between its current position and the best frog's position, and the worst frog will never jump over the best one (Fig. 5). Clearly, this frog leaping rule limits the local search space in each memetic evolution step.

This limitation might not only slow down the convergence speed, but also cause premature convergence. In nature, because of imperfect perception, the worst frog cannot locate exactly the best frog's position, and because of inexact action, the worst frog cannot jump right to its target position. Considering these uncertainties, we argue that the worst frog's new position is not necessary restricted in the line connecting its current position and the best frog's position. Furthermore, the worst frog could jump over the best one. This idea leads to a new frog leaping rule that extends the local search space as illustrated in Fig. 6:

$$D = r.c(X_b - X_w) + W \tag{8}$$

$$W = [r_1 w_{1,\max}, r_2 w_{2\max}, \ldots, r_s w_{s,\max}]^T \tag{9}$$

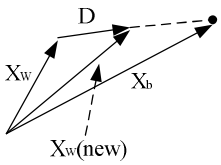

Fig. 5. The original frog leaping rule

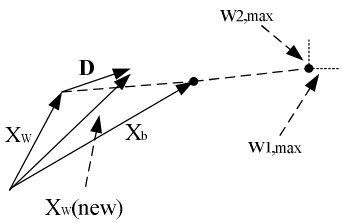

Fig. 6. The new frog leaping rule

$$X_w(new) = \begin{cases} X_w + D & if \|D\| \le D_{\max} \\ X_w + \dfrac{D}{\sqrt{D^T D}} D_{\max} & if \|D\| > D_{\max} \end{cases} \tag{10}$$

Where X_b, X_w and X_g are the frogs identified with the best, the worst and the global best fitnesses, respectively; r is a random number between 0 and 1; c is a constant chosen in the range between 1 and 2; $r_i(1<i<S)$ are random numbers between -1 and 1; $w_{i,\max}(1<i<S)$ are the maximum allowed perception and action uncertainties in the ith dimension of the search space; and $D_{\max}$ is the maximum allowed distance of one jump.

The flow chart of the local memetic evolution using the proposed frog leaping rule is illustrated in Fig. 7. The new frog leaping rule extends the local search space in each memetic evolution step; as a result it might improve the algorithm in term of convergence rate and solution performance provided that the vector $W_{max}=[w_{1,max}, \ldots, w_{S,max}]^T$ is appropriately chosen. However, if $\|W_{\max}\|$ is too large, the frog leaping rule will loss its directional characteristic, and the algorithm will become more or less random search. Hence, choosing a proper maximum

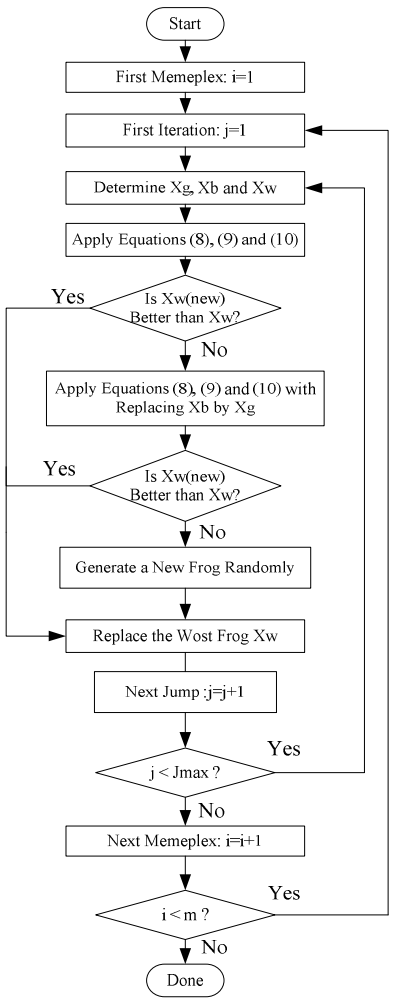

Fig. 7. The MSFLA flowchart

uncertainty vector is an issue to be considered for each particular optimization problem.

4. Simulation Results

4.1 Determination of parameters for MSFLA

The proposed MSFLA methodology is programmed in MATLAB running on an Intel w Core TM2 Duo Processor T5300 (1.73 GHz) PC with 1 GB RAM. The effect of MSFLA parameters on average fitness function (among 100 trials) is investigated. The colony size (N_C) was 100. Hundred independent trials have been made with 100 iterations per trial. The performance of the MSFLA also depends on the number of colonies. The parameters of MSFLA are selected based on the average fitness function, after a number of careful experimentation as following:

$$NC = 100;\ D_{max} = 0.6,\ r_i = 1.1;\ C=1.3;\ r=0.6.$$

4.2 Experimental result

The minimum fitness value evaluating process is depicted in Fig 8. According to it, the MSFLA is preferred method in terms of convergence. Thei MSFLA provides the correct answers with high accuracy in the initial iterations which makes the responding time of it extremely fast. The system proper values and damping ratio of mechanical modes with three different loading conditions are tabulated in Table 6. It is clear that the system with MSFLASVC is suffered from small damping factors (σ = -1.13, -1.37, -1.14) for light, normal, and heavy loading, respectively.

The coordinated controller shifts the electromechanical modes to the left of the S-plane, and consequently the values of the damping factors are considerably enhanced to -1.21, -1.36, -1.16 for light, normal, and heavy loading respectively. The damping ratios commensurate with coordinated controller are almost bigger than the uncoordinated ones. Thus, the proposed controller improves the damping features of electromechanical modes and system stability. The value of parameters for the different controllers using the MSFLA technique is shown in Table 7.

4.3 Light load condition

The vigorous performance of the coordinated controller

Table 6. Mechanical mode and ξ under different loading condition and controllers

Load	MSFLASVC	MSFLAPSS	Coordinated	Uncoordinated
Light	-1.65±j12.23, 0.1337	-3.56±j6.47, 0.4820	-3.76±j7.42, 0.4520	-3.27±j14.86, 0.2149
	-3.48±j9.86, 0.3328	-3.66±j5.65, 0.5436	-3.91±j6.65, 0.5068	-1.16±j8.45, 0.1360
	-1.13±j1.68, 0.5581	-0.75±j3.09, 0.2358	-1.21±j1.87, 0.5432	-0.59±j2.16, 0.2634
Normal	-1.19±j8.56, 0.1376	-3.63±j9.73, 0.3495	-3.11±j7.78, 0.3974	-3.23±j10.65, 0.2902
	-2.61±j6.57, 0.3691	-4.38±j7.63, 0.5000	-3.99±j8.19, 0.4379	-146±j9.68, 0.1491
	-1.37±j1.23, 0.7441	-0.53±j2.43, 0.2130	-1.36±j1.74, 0.7244	-0.36±j2.97, 0.1203
Heavy	-2.20±j6.06, 0.2136	-3.52±j5.26, 0.3920	-4.32±j8.40, 0.4573	-3.39±j9.92, 0.3233
	-1.62±j11.64, 0.1917	-3.36±j6.60, 0.4536	-3.72±j6.76, 0.4821	-1. 5±j11.52, 0.1283
	-1.14±j2.35, 0.4364	-0.71±j2.35, 0.2892	-1.16±j2.09, 0.4852	-0.34±j3.51, 0.0964

Table 7. Optimal PSSs and SVCs parameters for different controllers

Load	Coordinated design				Uncoordinated design			
	PSS1	PSS2	PSS3	SVC	PSS1	PSS2	PSS3	SVC
K	58.966	0.8896	1.3263	0.4581	22.9532	6.6325	7.0223	49.6236
T_1	0.1922	0.1791	0.2139	0.2232	0.3364	0.3602	0.2093	0.8203
T_3	0.2396	0.1236	0.1188	0.3811	0.3785	0.3896	0.2796	0.6098

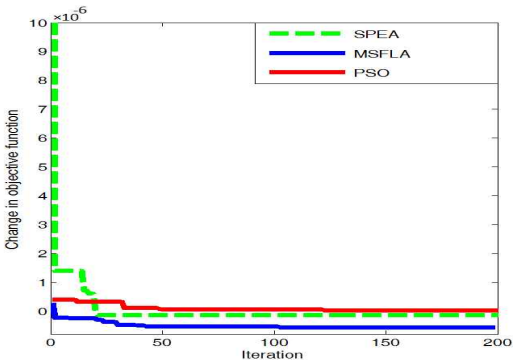

Fig. 8. Convergence profile for MSFLA, SPEA and PSO

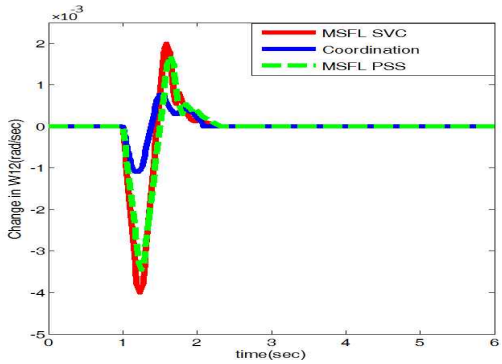

Fig. 9. Response of $\Delta\omega_{12}$ for light load condition

under disturbance is confirmed by implementing a three phase fault of 6 cycle duration at 1.0 s close to bus 7. The responses of Δω12, Δω23 and Δω13 for light loading condition are depicted in Figs. 9-11.

The ability of the proposed coordinated controller for diminishing the settling time and damping power system oscillations are verified in these figures. In addition, the settling time (T_s) of these oscillations is 1.94, 2.01, and 2.09s for coordinated controller, MSFLAPSS, and MSFLASVC respectively, and consequently the proposed coordinated controller is able to provide significant damping to the system oscillatory modes compared to MSFLAPSS, and MSFLASVC. Fig. 12 illustrates the response of $\Delta\omega_{12}$ for different optimization scheme. As it seen from the figure, MSFLA reveals better performance for designing the coordinated controller compared with SPEA and PSO.

4.4 Normal load condition

The responses of $\Delta\omega_{12}$, $\Delta\omega_{23}$ and $\Delta\omega_{13}$ owing to same disturbance for normal loading condition are shown in Figs. 13-15. The results reveal that the proposed coordinated controller has a superior ability for damping power system oscillations and intensifies the dynamic stability of power system. The settling time (T_s) of these oscillations are 1.85, 2.22, and 2.28s for coordinated controller, MSFLAPSS and MSFLASVC, respectively. Hence the designed controller is competent to provide significant damping to the system oscillatory modes and enlarge the power system stability constrain.

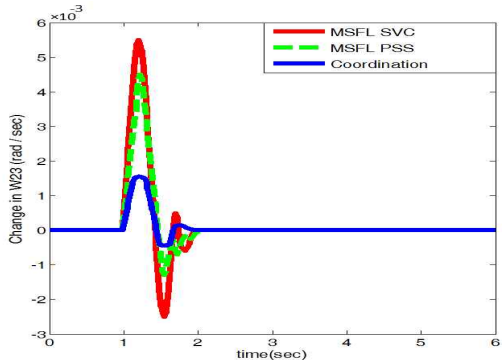

Fig. 10. Response of $\Delta\omega_{23}$ for light load condition

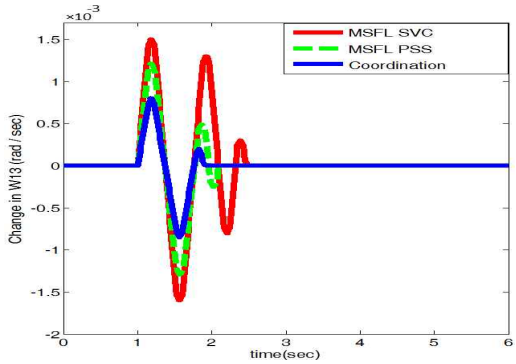

Fig. 11. Response of $\Delta\omega_{13}$ for light load condition

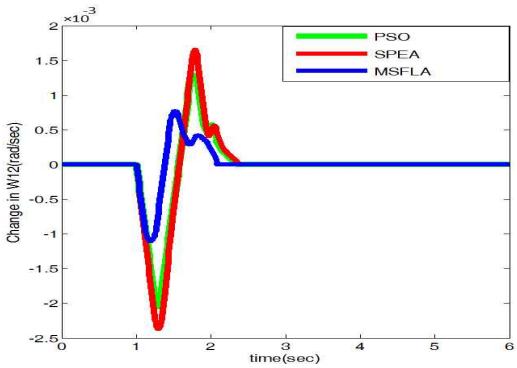

Fig. 12. Response of $\Delta\omega_{12}$ for different optimization techniques

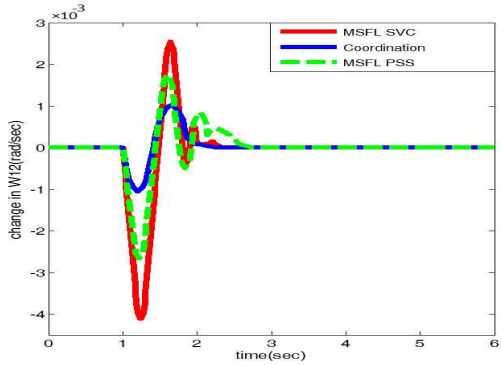

Fig. 13. Response of $\Delta\omega_{12}$ for normal load condition

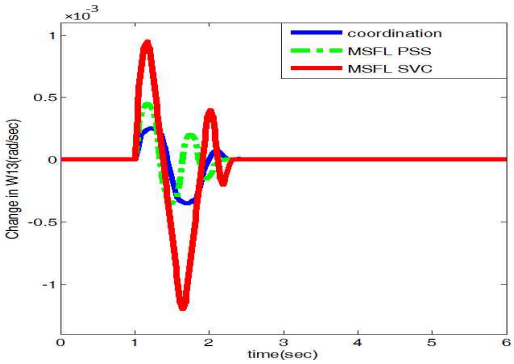

Fig. 14. Response of $\Delta\omega_{23}$ for normal load condition

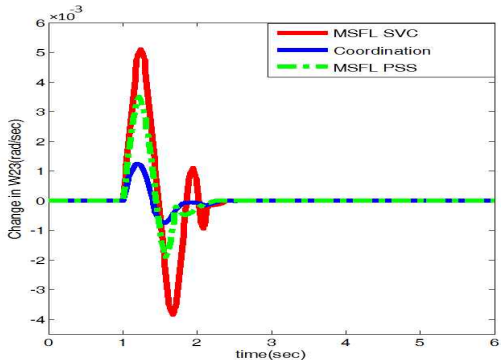

Fig. 15. Response of $\Delta\omega_{13}$ for normal load condition

Fig. 16 depicts a comparison between different schemes. The more competent and speedy convergence is seen using the proposed MSFLA scheme compared to SPEA and PSO.

4.5 Heavy load condition

The responses of $\Delta\omega_{12}$, $\Delta\omega_{23}$ and $\Delta\omega_{13}$ owing to same disturbance for heavy loading condition are illustrated in Figs. 17-19.

The coordinated controller reveals better damping features for low frequency oscillations. The settling times are 1.94, 2.02, and 2.43 s for coordinated controller, MSFLAPSS and MSFLASVC respectively. The supremacy of the simultaneous coordinated IMSFLASVC and MSFLAPSS over the uncoordinated designed controllers is demonstrated. The supremacy of proposed MSFLA in adjusting the coordinated controller in comparison with SPEA and PSO is shown in Fig. 20. Fig. 21 depicts the supremacy of the coordinated controller in diminishing the settling time and damping power system oscillations over

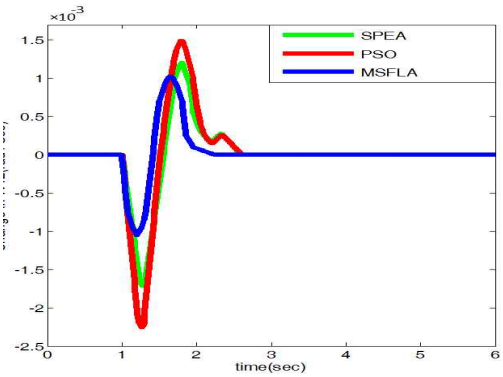

Fig. 16. Response of $\Delta\omega_{12}$ for different optimization techniques

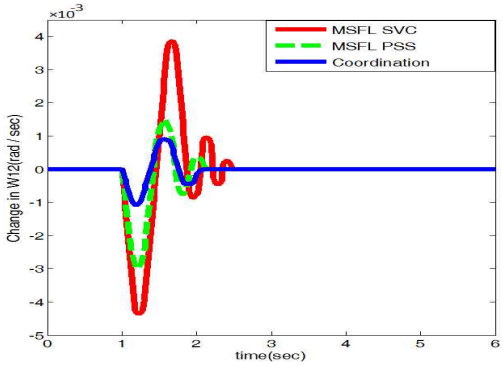

Fig. 17. Response of $\Delta\omega_{12}$ for heavy load condition

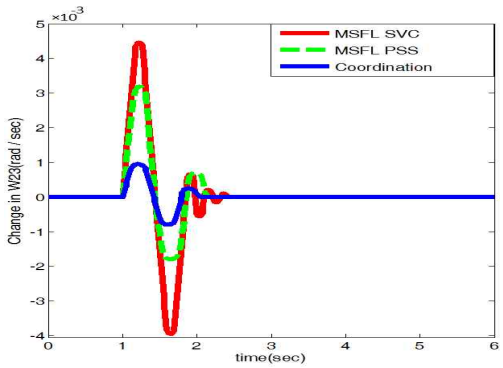

Fig. 18. Response of $\Delta\omega_{23}$ for heavy load condition

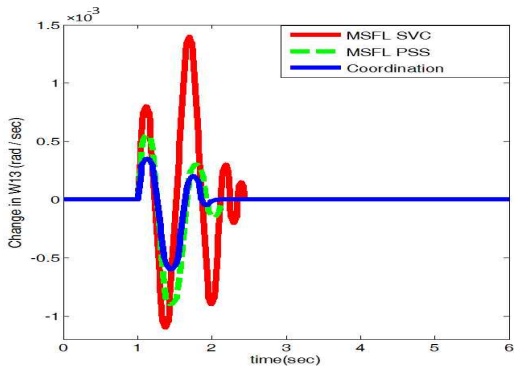

Fig. 19. Response of $\Delta\omega_{13}$ for heavy load condition

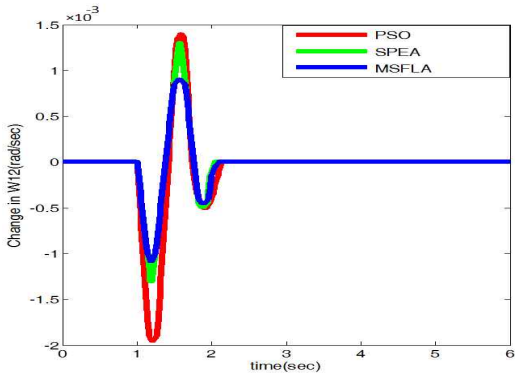

Fig. 20. Response of $\Delta\omega_{12}$ for different optimization techniques

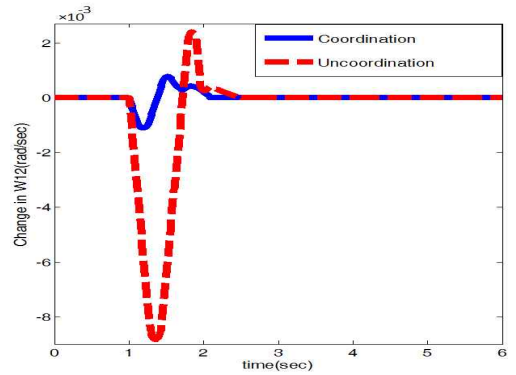

Fig. 21. Comparison between coordinated and uncoordinated design

the uncoordinated controller in response of $\Delta\omega_{12}$.

5. Conclusion

The subsequent adjustment of PSS and SVC parameters does not undertake the effectiveness of the PSS and SVC with variable load condition. This study is undertaken to propose a robust design technique for the simultaneous coordinated adjusting of the SVC and PSS damping controller in a multi-machine power system. The designing problem is converted to an optimization problem in which the speed deviations between generators are associated. The proposed MSFLA scheme is tested on a multi-machine power system under various disturbances and compared with PSO and SPEA based tuned PSS and SVC to demonstrate its strong ability. The most obvious findings from this study are as follow:

1. The proposed MSFLA scheme for tuning SVC and PSSs is easy to implementation without additional computational complexity;
2. The convergence rate of high accuracy and speed are notably improved;
3. Power system stability and also power transfer ability are extended via the proposed scheme.

References

[1] M. Abido, Y. Abdel-Magid, "Coordinated design of a PSS and an SVC-based controller to enhance power system stability," *Int J Electr Power Energy Syst*, vol. 25, pp. 695-704, 2003.

[2] N. G. Hingoran and L. Gyugyi, "Understanding FACTS, Concepts and Technology of Flexible AC Transmission System," *Institute of Electrical and Electronics Engineering, Inc*., New York, 2000.

[3] Y. Abdel-Magid, M. Abido, "Optimal multiobjective design of robust power system stabilizers using genetic algorithms," *IEEE Trans Power Syst*, vol. 18, no. 3, 2003, pp. 1125-1132.

[4] Y. Abdel-Magid, M. Abido, A. Mantawy, "Robust tuning of power system stabilizers in multi machine power systems," *IEEE Trans Power Syst*, vol. 15, no. 2, 2000, pp. 735-40.

[5] M. Abido, "Robust design of multi-machine power system stabilizers using simulated annealing," *IEEE Trans Energy Convers*, vol. 15, no. 3, 2003, pp. 297-304.

[6] M. Abido, Y. Abdel-Magid, "Optimal design of power system stabilizers using evolutionary programming," *IEEE Trans Energy Convers*, vol. 17, no. 4, 2000, pp. 429-36.

[7] M. Furini, A. Pereira, P. Araujo, "Pole placement by coordinated tuning of power system stabilizers and FACTS POD stabilizers," *Int. J. Electr. Power Energy Syst,*vol. 33, no. 3, 2011, pp. 615-22.

[8] M. Haque, "Best location of SVC to improve first swing stability of a power system," *Int. J. Electr. Power Syst. Res,*vol. 77, no. 10, 2007, pp. 1402-9.

[9] Y. Chang, Z. Xu, "A novel SVC supplementary controller based on wide area signals," *Int. J. Electr. Power Syst*, Res,vol. 77, no. 12, 2007, pp. 1569-74.

[10] E. Ali, "SVC design for power system stabilization using bacteria foraging optimization algorithm," *in Proc. of MEPCON2009 Conference, Egypt*, December, 2009.

[11] Y. Yuan, G. Li, L. Cheng, Y. Sun, J. Zhang, P. Wang, "A phase compensator for SVC supplementary control to eliminate time delay by wide area signal input," *Int. J. Electr. Power Energy Syst*, vol. 32, no. 3, 2010, pp. 163-9.

[12] E. Zhijun, D. Fang, K. Chan, S. Yuan, "Hybrid simulation of power systems with SVC dynamic phasor model," *Int. J. Electr. Power Energy Syst*, Vol. 31, No. 5, 2009, pp. 175-8.

[13] S. Panda, N. Patidar, R. Singh, "Simultaneous tuning of SVC and power system stabilizer employing real-coded genetic algorithm," Int. *J. Electr. Electron. Eng*. Vol.4, No. 4, 2009, pp. 240-7.

[14] X. Bian, C. Tse, J. Zhang, K. Wang, "Coordinated design of probabilistic PSS and SVC damping controllers," *Int. J. Electr. Power Energy Syst,* Vol.33, No.3, 2011 pp. 445-52.

[15] M. Furini, A. Pereira, P. Araujo, "Pole placement by coordinated tuning of power system stabilizers and FACTS POD stabilizers," *Int. J. Electr. Power Energy Syst,* Vol.33, No.3, 2011 pp. 615-22.

[16] E. Ali, S. Abd-Elazim, "Coordinated design of PSSs and TCSC via bacterial swarm optimization algorithm in a multimachine power system," *Int. J. Electr. Power Energy Syst*, Vol. 36, No. 1, 2012 pp. 84-92.

[17] J. Kennedy, R. C. Eberhart, "Particle swarm optimization", *Proc. Int. Conf. on neural networks*, pp. 1942-1948, 1995, Perth, Australia.

[18] H. Yassami, A. Darabi, S.M.R. Rafiei, "Power system stabilizer design using Strength Pareto multi-objective optimization approach," *Int. J. Electr. Power Energy Syst,*Vol. 80, 2010, pp. 838-846.

[19] P. Kundur, M. Klein, G. Rogers, M. Zywno, "Application of power system stabilizers for enhancement of overall system stability," *IEEE Trans. Power Syst,* Vol. 4, No. 2, 1989, pp. 614-626.

[20] Anderson PM, Fouad AA, "Power System Control and Stability," Iowa: Iowa State University Press; 1977.

[21] S. M. Abd-Elazim, "Comparison between SVC and TCSC Compensators on Power System Performance," Master Thesis, 2006, Zagazig University, Egypt.

[22] S. Jalilzadeh, M. Azari, "Robust tuning of PSS controller to enhance power system stability," *Proc. of ICACEE2012 Conference*, Manila, Philippines, 2012.

Mohsen Darbian He received his B.Sc. and M.Sc. degrees both in electrical engineering from Islamic Azad University (Abhar branch) and University of Zanjan, Iran, in 2010 and 2013, respectively. He is a Ph.D student in Electrical Engineering, at University of Zanjan, Iran.

Abolfazl Jalilvand He received B.Sc. in electrical engineering from Shahid Beheshti University, Iran, in 1995; then M.Sc. and Ph.D. degrees from University of Tabriz, Iran, in Power Engineering and Control Engineering in 1998 and 2005, respectively. Currently, he is an Associate Professor at university of Zanjan, Iran.